Simple, Robust Autonomous Grasping in Unstructured Environments

Aaron M. Dollar, *Student Member, IEEE*, and Robert D. Howe, *Member, IEEE*

Abstract—The inherent uncertainty associated with unstructured grasping tasks makes establishing a successful grasp difficult. Traditional approaches to this problem involve hands that are complex, fragile, require elaborate sensor suites, and are difficult to control. In this paper, we demonstrate a novel autonomous grasping system that is both simple and robust. The four-fingered hand is driven by a single actuator, yet can grasp objects spanning a wide range of size, shape, and mass. The hand is constructed using polymer-based Shape Deposition Manufacturing, with joints formed by elastomeric flexures and actuator and sensor components embedded in tough rigid polymers. The hand has superior robustness properties, able to withstand large impacts without damage and capable of grasping objects in the presence of large positioning errors. We present experimental results showing that the hand mounted on a three degree of freedom manipulator arm can reliably grasp 5 cm-scale objects in the presence of positioning error of up to 100% of the object size and 10 cm-scale objects in the presence of positioning error of up to 33% of the object size, while keeping acquisition contact forces low.
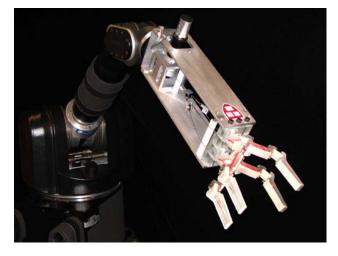
Fig. 1. Four-fingered, underactuacted SDM hand mounted on a Whole-Arm Manipulator (Barrett Technology Inc., Cambridge, MA, USA). A single motor drives all eight joints of the hand

I. INTRODUCTION

Grasping and manipulating objects in unstructured environments, where object properties are not known *a priori* and sensing is prone to error, is one of the central challenges in robotics. The uncertainty in the relationship between the object and gripper makes it difficult to control contact forces and establish a successful grasp.

One approach to dealing with this uncertainty is through compliance, so that positioning errors do not result in large forces and the grasper conforms to the object. Compliance has most often been implemented through control of manipulator impedance, based on active use of joint sensors for position, velocity and force/torque [1-3]. However, carefully designed *mechanical* compliance in the finger structure can allow the gripper to passively conform to a wide range of objects while minimizing contact forces.

Compliance conveys two key advantages for robotic grasping: adaptability and robustness. We take advantage of the adaptability inherent with compliance and enhance it by

Fig. 2. Four-fingered SDM grasping a volleyball, a wine glass filled with water, a compact disc, and a large wood block.

incorporating further adaptability in the form of underactuation. An underactuated hand has fewer actuators than degrees of freedom, and therefore demonstrates adaptive behavior. In these hands, the transmission design allows motion of other joints to continue after contact occurs on a coupled link, allowing the hand to passively adapt to
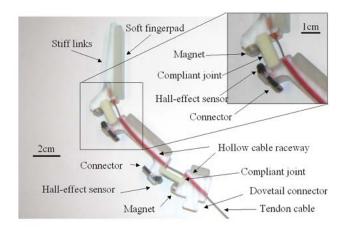
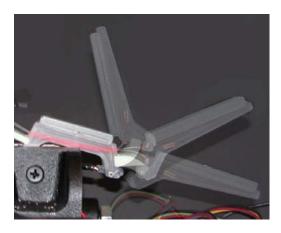Fig. 3. Details of finger parts and placement of components.

Fig. 4. Superimposed photograph of joint deflection and link motion for three positions across the travel range of the distal joint of the fingers. The center image is the rest position.

the object shape.

Unintended contact that often occurs in unstructured grasping tasks can result in large contact forces unless the gripper is compliant. This contact can occur due to sensing uncertainty in unstructured environments, but can also happen in laboratory experiments, particularly in the debugging phase. Researchers are often reluctant to risk crashes with expensive multi-degree-of-freedom robot hands, so implementations must be carefully validated and experimental scope must be limited.

Designing durable robots, although rarely addressed in robotics research, is essential in industrial, space, and military applications. Examples include iRobot's "PackBot" [4], University of Minnesota's "Scout" family of launchable robots [5], and MIT manipulator arms for the NASA/JPL Pathfinder and Surveyor Mars missions [6]. In research, this durability would expand the type of experimental tasks that can be reasonably attempted and speed implementation due to the reduced need for careful validation of programs.

We begin this paper by describing the design, fabrication, and evaluation of a robust four-fingered grasper (Figs. 1 and 2) built using Shape Deposition Manufacturing (SDM) [7-9]. This process uses polymeric materials to simultaneously create the rigid links and compliant joints of the gripper,
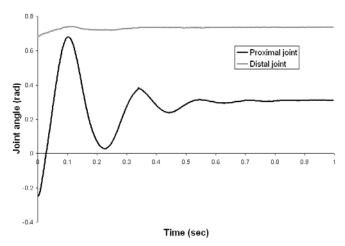

Fig. 5. Joint response of the SDM finger to a tip step displacement released at time=0.

with embedded sensing and actuation components. In addition to simplifying the construction process, the result is an extremely robust gripper, fully functional after impacts and other large loads due to unintended contact. We then describe the results of an experimental study in which we evaluate the ability of our grasping system to autonomously grasp a number of target objects in the presence of varying levels of positional error.

II. SDM HAND DESIGN

To provide both adapatability and robustness, our hand, featuring passively compliant joints, was fabricated using polymer-based Shape Deposition Manufacturing (SDM) [7-9] (Figs. 1 and 2). SDM is an emerging layered manufacturing technique with which the rigid links and compliant joints of the gripper are created simultaneously, with embedded sensing and actuation components. Elastomeric flexures create compliant joints, eliminating metal bearings, and tough rigid polymers fully encase the embedded components, eliminating the need for seams and fasteners that are often the source of mechanical failure.

A. Finger design

Fig. 3 diagrams the parts of the SDM finger. The concave side of each link contains a soft fingerpad to maximize friction and contact area, thereby increasing grasp stability [10,11]. Links are connected via elastomer joint flexures, designed to be compliant in the plane of finger motion and stiffer out of plane. Fig. 4 shows the behavior of the distal finger joint through its range of motion.

The polyurethane used for these joints demonstrates significant viscoelastic behavior, which is necessary to reduce the severity of joint oscillations and permit the use of low joint stiffness. Figure 5 shows the joint response of the SDM finger to a large step displacement of the fingertip, released at time t=0. Note that the oscillations are negligible after less than 1 second. In a conventionally-assembled grasper with metal springs, oscillations due to large step displacements were found to persist for tens of seconds after
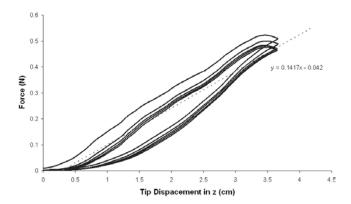
Fig. 6. Force-deflection curve of the tip of the SDM finger with linear trendline. The data represents five cycles of tip motion.

release.

Due to the molding process used to create them, the SDM fingers, with embedded sensors and actuation components, are a single part weighing 39 grams, with no fasteners or adhesives. This is in contrast to a similar grasper fabricated with conventional metal prototyping techniques used in our previous work, which had 60 parts total, 40 fasteners, and weighed 200 grams [12].

B. Finger compliance and robustness

Fig. 6 shows the force generated at the tip of the fingers due to displacement in the out-of-plane direction. The tip was displaced at a rate of approximately 1 cm/sec while mounted on an actuated linear slide mechanism, with force measured by a multi-axis force/torque sensor. This data represents force generated due to motion of the tip across the tested range and back for a total of five cycles, low-pass filtered with a cut-off frequency of 1 Hz, to remove sensor noise. Note the hysteresis in the curves and the force relaxation due to viscoelasticity.

This result shows that the SDM fingers, while exhibiting very low tip stiffness, can also undergo large deflections while remaining completely functional. In the test shown in Fig. 6, the tip was displaced more than 3.5 cm in the out-of-plane direction (approximately 20 degrees) without any degradation of mechanical properties. The advantages of this property are clear when considering the usual result of unplanned contact during use of traditional research robotic hands.

To give a sense of the robustness of the mechanism to impacts and other potentially harmful loads, a number of more informal tests were performed. An SDM finger was repeatedly dropped from a height of over 15m (50') onto a stone floor, without significant damage. The fully-assembled hand has been hit repeatedly with a hammer, fingers jammed against objects, and even used underwater, without any degradation of performance (see accompanying video).

1) Kinematic and stiffness configuration

The preshape and stiffness characteristics of the hand were determined based on the results of an optimization study. In this simulation, the joint rest angles and joint stiffness ratio of the fingers were varied and the performance analyzed to maximize the allowable uncertainty in object location (successful grasp range) and size as well as minimize contact forces.

The grasping model combined the inverse kinematics of the mechanism, torque balances for each joint, work balance, and equations describing the geometry of the grasper and object. MATLAB (The Mathworks, Natick, MA, USA) was used to numerically solve these systems of equations and allow for the performance of the grasper to be tested over a wide range of variations in grasper parameters.

In order to reduce the parameter space and allow for detailed analysis of parametric trade-offs, a simplified version of our hand was examined: a planar, two-fingered, four-jointed gripper with links that are rigid lines between compliant rotational joints. The object to be grasped was assumed to be circular (a frequent assumption in the grasping literature, and a reasonable approximation for many objects), and sufficiently massive such that the gripper contact forces do not displace or rotate it. We ignored inertial effects and assumed quasi-static conditions.

Based on the results of this study, the preshape configuration $\varphi_1=25°$ (angle with the horizontal in Fig.) and $\varphi_2=45°$ (angle with the proximal link) was chosen for our final finger design. In addition, the results showed that the proximal joint should be much stiffer than the distal joint, keeping the grasping surface concave and contact forces low. These angles and stiffnesses were shown to enable grasping of the widest range of object sizes with the greatest amount of uncertainty in object position, while also exhibiting low average contact force, reducing the likelihood of displacing or damaging the object. Additionally, these results were confirmed experimentally by testing the performance of a reconfigurable aluminum grasper as joint rest angles and stiffnesses were varied. See [12] for further details of these studies.

C. Actuation

For actuation, each finger has a pre-stretched, nylon-coated stainless steel cable anchored into the distal link, and running through low-friction nylon 11 tubing to the base (Fig. 3). The grasper is unactuated until contact is made with the target object and a successful grasp is predicted based on the available sensory information. Before actuation, the tendon cable, which is in parallel with the compliant joints, remains slack and the finger is in its most compliant state. This method permits the use of actuators that are not backdrivable and prevents the inertial load of the actuator from increasing the passive stiffness. After actuation, the stiff tendon takes much of the compliance out of the fingers, resulting in a stiffer grasp with greater stability.

A single actuator drives the four fingers (eight joints) of the hand. This property not only makes the gripper simpler and lighter, but it also allows the gripper to be self-adapting
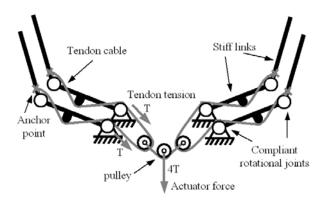
Fig. 7 Actuation schematic of the hand

to the target object. Fig. 7 details the actuation scheme, by which motion of the distal links can continue after contact on the coupled proximal links occurs, allowing the finger to passively adapt to the object shape. Additionally, the pulley design in this scheme allows the remaining fingers to continue to enclose the object after the other fingers have been immobilized by contact, ensuring that an equal amount of tension is exerted on each tendon cable, regardless of finger position or contact state.

The four fingers are staggered on the palm to allow them to completely close without interfering with one another.

1) Joint coupling design

The joint coupling scheme employed on each finger was determined based on the results of another optimization study. In this simulation, the joint coupling scheme (ratio of torque applied at the distal/proximal joints divided by the stiffness ratio of the joints) was varied in order to maximize the allowable uncertainty in object location (successful grasp range) and size as well as minimize contact forces. The simulation approach followed the kinematics and stiffness study described in section II A. 1 above.

The results of this study suggested that, to keep unbalanced object forces low, torque ratio (ratio of torque applied at the distal/proximal joints divided by the stiffness ratio of the joints) should be as large as possible. However, as torque ratio increases, the position range in which an object can be successfully grasped (maximum allowable positioning error) is decreased.

This tradeoff in force versus successful grasp range can be weighed by considering the quality of the sensory information available for the grasping task. For a task in which the location of the target object can be accurately sensed, the torque ratio can be large, since the gripper can be reliably centered on the object. However, for tasks in which sensory information is poor, the positioning of the gripper is subject to large errors, requiring that the chosen torque ratio should allow for large positioning errors. Since our hand is intended for grasping in unstructured environments resulting in large expected positioning errors, we chose a lower torque ratio $((\tau_2/\tau_1)/(k_2/k_1)=0.6)$. See [13] for further details of this study.

III. EXPERIMENTAL SETUP

In order to determine the effectiveness of our hand at grasping objects in unstructured conditions, we experimentally evaluated the ability of the hand to grasp three-dimensional objects in a three-dimensional environment with large errors in the sensed target object location and a very simple control scheme. Specifically, we examine the amount of positioning error allowable in order to obtain a stable grasp on the object, and record the forces on the object during the grasping task.

A. Robot manipulator

The SDM Hand was mounted on a low-impedance robotic arm (Whole-Arm Manipulator (WAM), Barrett Technology, Cambridge, MA, USA) for positioning (Fig. 1). Only three of the four joints of the WAM were utilized for a total of three positioning degrees of freedom: the base roll, shoulder pitch, and elbow pitch. Since there is no wrist, orientation of the hand was not controlled and was determined based on the kinematics of the manipulator at the target position.

The WAM was controlled using a 1000 Hz servo loop running on a DSP (DS1103 PPC, dSPACE Inc., Novi, MI). The desired position was achieved using a PID controller with gains chosen so that the overall stiffness was dominated by the remote environment stiffness. To increase performance and allow for the use of lower gains, the robot controller uses a feedforward model of the forces on the arm (before contact with the object), including compensation for torque ripple, gravity, and friction.

B. Workspace

Target objects were mounted on a 6-axis force/torque sensor with a resolution of 0.1 N (Gamma model, ATI Industrial Automation, Inc, Apex, NC, USA). Objects were mounted to the force sensor via a square peg, such that position and orientation in the plane were fixed, yet the object could be lifted up out of the mount after grasping. Only contact forces in the plane of the workspace table were recorded, and torques were ignored. Robot inertia was kept small by using low accelerations during exploration, reducing the task to nearly quasi-static conditions.

Two objects were tested at three configurations, for a total of six conditions (Fig. 8). The objects were a cylindrical PVC tube with a radius of 24mm (0.3 times the grasper link length l), and a wooden block with a 84 mm x 84 mm cross section (equivalent to 0.75 times the grasper link length l). This block was oriented such that a flat side was approximately normal to the approach direction. As reflected in Fig. 8, the difference in object position served to change the approach angle of the grasper with respect to the long axis of the objects.

IV. EXPERIMENTAL PROCEDURE

The experiment begins by finding the 'zero position' for the particular object and location. This position was taken as
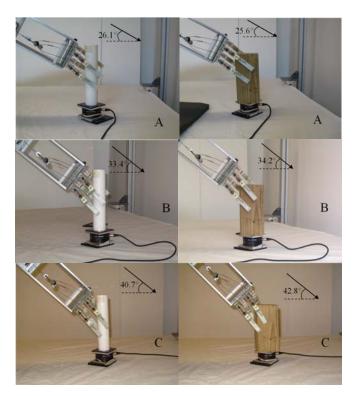
Fig. 8. Two target objects (PVC cylinder of radius 24mm and wood block with square cross-section 90mm side length) at three locations (A, B, and C). Note the differences in approach angle for the locations, the main factor affecting the force and grasp space results.

the point at which the hand contacts the object without any deflection, centered on the object; this represents the positioning of the hand under perfect visual sensing (hand is centered on the object) and perfect contact sensing (stopping the manipulator at the instant of initial contact). The y direction was taken along the line lying between the robot origin and the center of the object, normal to the direction of gravity. The x direction is normal to the y direction, also normal to the direction of gravity (the z direction). The robot was positioned at 10mm increments from the zero position in the positive x (symmetry in the positive and negative x direction was assumed) and positive and negative y directions (grasping behavior is not symmetric in y). Forces on the object and whether the grasp was successful were recorded for each position. The vertical position of the hand was kept constant across object positions (Fig. 8).

The manipulator joint angles were calculated using the inverse kinematics of the robot and rounded to the nearest tenth of a degree. The forward kinematics were then recomputed, updating the array of tested configurations. The resulting deviations from the target grid are less than 1 mm in every direction.

For each position, the robot moves to within a tenth of a degree of the target configuration at each joint. The robot then initiates the grasp by driving the grasping motor to a preset torque (stall) and thus closing all fingers. When an encoder indicates motor stall, the motor current is reduced to a small amount required to prevent backdriving of the motor

due to the tendon force. The arm then attempts to lift the object vertically out of the force sensor mount. This simple, strictly feedforward hand control mode is used to evaluate the benefits of the optimized passive compliance and adaptive coupling approach to hand design. The sensors on the hand are not used in this study.

Each location on the (x,y) grid of positions was tested three times, and the force results averaged. Force was recorded at 1000 Hz during the experiment. Data from the force sensor was filtered by taking the median of the previous 20 force samples (0.02 s).

A grasp was deemed successful if the object was lifted vertically out of the force sensor mount a distance of 150mm, and the grasp appeared to be stable (i.e. no slippage of the object was visually observed). Grasps could fail at a given position for a number of reasons: passive contact force pushes the object out of the sensor mount or pushes the sensor out of the table mount, too few fingers make contact with the object, or an imbalance of forces on the object due to undesirable positioning leads to it being ejected from the grasp.

V. RESULTS

Figs. 9 and 10 show the results of the force and successful grasp space study for the two objects at three configurations each. The left column ($F_{approach}$) indicates the magnitude of the maximum force applied to the object during the approach phase of the grasp (hand has not yet been actuated). The right column (F_{grasp}) indicates the magnitude of the maximum force applied to the object during the grasp phase (fingers are closing in on the object, before motion of the arm to lift the object out of the sensor mount).

The various points on the plots that are labeled correspond to interesting or otherwise demonstrative configurations. A description of the grasping behavior at these points is given in Tables I and II.

The boundary of these plots is a rough approximation of the successful grasp range (the amount of allowable positioning error resulting in a successful grasp) for the particular object and position. Note that the successful grasp range is significantly affected by the approach angle of the hand. The steeper the approach angle, the less likely enough fingers will be in contact with the object to create a stable grasp (Fig. 8).

The results show that the PVC cylinder (48mm diameter) could be successfully grasped at positions up to 50mm from the center in x, and +20mm,-30mm in y, for a total allowable positioning error of over 100% of the object size. Not surprisingly, shallow (more horizontal) hand orientations lead to larger successful grasp ranges. For the wooden block (84mm x 84mm cross section), positioning errors of up to 20mm from the center in x, and +20mm,-20mm in y resulted in a successful grasp, for a total allowable positioning error of over 33% of the object size.

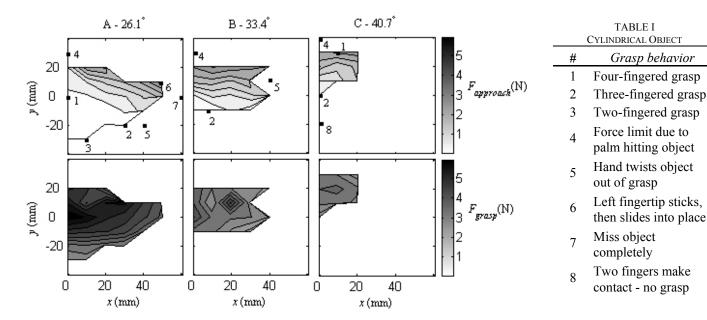In general, the shape and orientation of these objects lend

Fig. 9. Forces on the PVC cylinder object during the approach (top row) and grasp (bottom row) phases for the three object locations (columns). Labeled configurations correspond to the behavior indicated in Table I.

TABLE I
CYLINDRICAL OBJECT

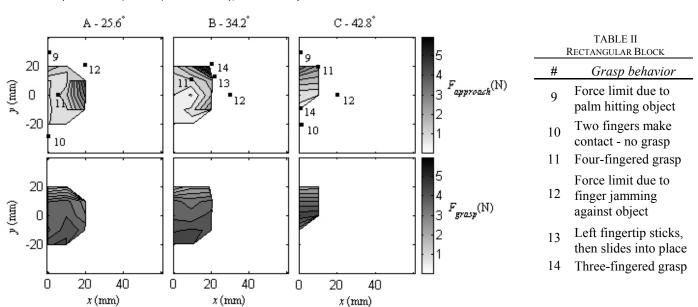| #	Grasp behavior
1	Four-fingered grasp
2	Three-fingered grasp
3	Two-fingered grasp
4	Force limit due to palm hitting object
5	Hand twists object out of grasp
6	Left fingertip sticks, then slides into place
7	Miss object completely
8	Two fingers make contact - no grasp

Fig. 10. Forces on the wooden block during the approach (top row) and grasp (bottom row) phases for the three object locations (columns). Labeled configurations correspond to the behavior indicated in Table II.

TABLE II
RECTANGULAR BLOCK

#	Grasp behavior
9	Force limit due to palm hitting object
10	Two fingers make contact - no grasp
11	Four-fingered grasp
12	Force limit due to finger jamming against object
13	Left fingertip sticks, then slides into place
14	Three-fingered grasp

themselves better to a shallow or horizontal hand orientation, aligning the axis of the power grasp configuration with the major axis of the object. For this reason, additional manipulator or wrist degrees of freedom can greatly expand the amount of allowable positioning uncertainty across the manipulator workspace, particularly if the orientation of the major axis of the object can be estimated.

It can be seen from the contours that, in general, F_{pass} increases with increasing y. This is expected since motion forward increases the passive deflection of the joints due to contact, increasing the force. The apparent discrepancy with this trend seen in Fig. 10 A, is simply an artifact of the sampling and contour generation. With decreasing y, the force goes to zero, as passive contact with the object is lost.

As x increases, F_{pass} increases as well. This is particularly significant in the wooden block cases, where the forward-most finger first "jams" against the face of the block, eventually slipping to the side, enabling a successful grasp. As x increases, the amount of "slip" of this finger necessary for a successful grasp increases, thereby increasing the passive force. Note that, as in this example, the maximum passive force often occurs before the hand has reached the target position.

The trends in the F_{grasp} plots can be largely explained in the following way: For each object there is some "grasp
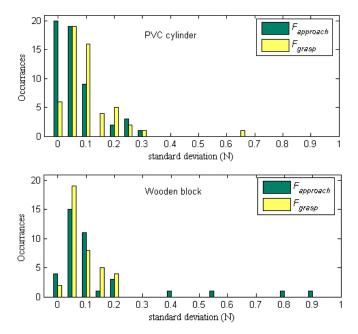
Fig. 11. Histograms of the standard deviation of the force measurements for the PVC cylinder (top) and wooden block (bottom).

equilibrium" configuration, located approximately in the center of the grasp in the y direction, where the forces on the object balance. Since the zero position for each object was based on the location of the front of the object and not the center, the size of the object affects the grasp equilibrium position. This position is in negative y for smaller objects (i.e. the object is "too close" to the base of the hand at the zero position) and positive y for larger objects (i.e. object is "too far" from the base at the zero position). Positions far away from the equilibrium position will result in high forces.

Fig. 11 shows histograms of the standard deviation of the force measurements (three samples at each configuration) for the two objects. Note that the total number of samples are different for the two objects: 38 for the wooden block and 54 for the PVC cylinder.

It can been seen from the plots that, while the values of standard deviation are typically less than the sensor resolution (0.1N), there are a number of instances of large variation in the force measurements between trials, particularly during the approach phase for the wooden block. These instances occur at positions close to transition points between general grasp behaviors. For instance, when grasping the wooden block, if the tip of a finger is very close to one of the edges, slight changes in hand or robot configuration can lead to drastically different behaviors (jamming against the object face vs. gently slipping to the side).

VI. Conclusions and Future Work

The intention in this study is not to suggest the details of a procedure to grasp objects in an unstructured environment, or to advance a particular grasper configuration. Rather, we

empirically demonstrate that optimized passively compliant joints and adaptive coupling can allow the grasping system to adapt to the large positioning errors that can occur in these types of tasks. Even with simplified positioning and control (three degree of freedom arm with no wrist, a single actuator for the eight joints of the hand, and feedforward hand control), we are able to grasp 5 cm-scale objects in the presence of positioning error of up to 100% of the object size and 10 cm-scale objects in the presence of positioning error of up to 33% of the object size.

There are a number of logical extensions to this work. The degree of autonomy demonstrated here can easily be expanded upon by utilizing the sensory information available from the joint angle and contact sensors already included in the hardware of the hand. This information, used in conjunction with an approximate model of object size and location from basic visual sensing, will make the grasping task even more robust to variations in object shape and position. Additional orientation degrees of freedom will also improve the performance by better relating hand and object geometry.

The ability of the hand to perform complicated grasping tasks can be further evaluated by operating the manipulator in teleoperation mode, allowing for more precise and dexterous positioning in order to perform more sensitive tasks. Preliminary study of use of this mode (see accompanying video) indicates that a broad range of difficult tasks can be performed even with simple kinematics and hand control.

References

[1] K. J. Salisbury, "Active stiffness control of a manipulator in Cartesian coordinates," 19th IEEE Conf. Decision and Control, pp..95-100, 1980.

[2] M. R. Cutkosky and I. Kao, "Computing and controlling the compliance of a robotic hand," IEEE Transactions on Robotics and Automation, vol. 5 (2), pp. 151-165, 1989.

[3] J. P. Desai and R. D. Howe, "Towards the development of a humanoid arm by minimizing interaction forces through minimum impedance control," Proceedings of the 2001 IEEE Int. Conf. on Robotics and Automation, pp. 4214-4219, 2001.

[4] iRobot Corporation, Government and Industrial Robotics Division, Burlington, MA, USA, (www.irobot.com/governmentindustrial).

[5] D. F. Hougen et al., "A Miniature Robotic System for Reconnaissance and Surveillance," Proceedings of the 2000 IEEE International Conference on Robotics and Automation, pp. 501-507, San Francisco, CA, April 2000.

[6] D. A. Theobald et al., "Autonomous Rock Acquisition," Proceedings of the AIAA Forum on Advanced Developments in Space Robotics, Madision, Wisconsin, August, 1-2, 1996.

[7] R. Merz, F. B. Prinz, K. Ramaswami, M. Terk, L. Weiss, "Shape Deposition Manufacturing," *Proceedings of the Solid Freeform Fabrication Symposium*, University of Texas at Austin, August 8-10, 1994.

[8] J. E. Clark, J. G. Cham, S. A. Bailey, E. M. Froehlich, P. K. Nahata, R. J. Full, M. R. Cutkosky, "Biomimetic design and fabrication of a hexapedal running robot," Proceedings of the 2001 International Conference on Robotics and Automation, Seoul, Korea, 2001.

[9] A. M. Dollar and R. D. Howe, "A Robust Compliant Grasper via Shape Deposition Manufacturing," ASME/IEEE Transactions on Mechatronics, vol. 11(2), 2006.

[10] K. B. Shimoga, A. A. Goldenberg, "Soft materials for robotic fingers," *Proceedings of the 1992 IEEE International Conference on Robotics and Automation*, pp. 1300-1305, 1992.

[11] M. R. Cutkosky, J. M. Jourdain, P. K. Wright, "Skin materials for robotic fingers*," Proceedings of the 1987 IEEE International Conference on Robotics and Automation*, pp. 1649-1654, 1987.

[12] A. M. Dollar and R. D. Howe, "Towards grasping in unstructured environments: Grasper compliance and configuration optimization," Advanced Robotics, vol. 19 (5), pp. 523-544, 2005.

[13] A. M. Dollar and R. D. Howe, "Joint Coupling Design of Underactuated Grippers," Proceedings the 30th Annual ASME Mechanisms and Robotics Conference, 2006 International Design Engineering Technical Conferences (IDETC), Philadelphia, PA, Sept. 10-13, 2006.